

#### **OPEN ACCESS**

EDITED BY
Zhen Xu,
Chinese Academy of Sciences (CAS), China

Mengmeng Zhao, Foshan University, China Avinash Premraj, Management of Scientific Centers & Presidential Camels, United Arab Emirates

\*CORRESPONDENCE
W. Ted Allison
Led.allison@ualberta.ca

RECEIVED 04 August 2025 REVISED 31 October 2025 ACCEPTED 05 November 2025 PUBLISHED 26 November 2025

#### CITATION

Fox APD, Lee TS, Mithaiwala SN, Pollock NM, Latif A, Bhavsar AP and Allison WT (2025) Adopting orphan receptors: zebrafish Tlr4 homologs mediate responses to group IX/X transition metals. Front. Immunol. 16:1679375. doi: 10.3389/fimmu.2025.1679375

# COPYRIGHT

© 2025 Fox, Lee, Mithaiwala, Pollock, Latif, Bhavsar and Allison. This is an open-access article distributed under the terms of the Creative Commons Attribution License (CC BY).

The use, distribution or reproduction in other forums is permitted, provided the original author(s) and the copyright owner(s) are credited and that the original publication in this journal is cited, in accordance with accepted academic practice. No use, distribution or reproduction is permitted which does not comply with these terms.

# Adopting orphan receptors: zebrafish Tlr4 homologs mediate responses to group IX/X transition metals

Aaron P.D. Fox<sup>1</sup>, Tracy S. Lee<sup>2</sup>, Sakina N. Mithaiwala<sup>1</sup>, Niall M. Pollock<sup>1</sup>, Asna Latif<sup>2</sup>, Amit P. Bhavsar<sup>2,3</sup> and W. Ted Allison<sup>1,4</sup>\*

<sup>1</sup>Department of Biological Sciences, Faculty of Science, University of Alberta, Edmonton, AB, Canada, <sup>2</sup>Department of Medical Microbiology and Immunology, Faculty of Medicine & Dentistry, University of Alberta, Edmonton, AB, Canada, <sup>3</sup>Department of Pharmacology, Faculty of Medicine & Dentistry, University of Alberta, Edmonton, AB, Canada, <sup>4</sup>Department of Medical Genetics, Faculty of Medicine & Dentistry, University of Alberta, Edmonton, AB, Canada

TLR4 is the prototype immune receptor and central to infection defense via detecting lipopolysaccharide (LPS). Surprisingly, the impacts of LPS upon the TLR4 homologs in zebrafish, an important animal model, are equivocal and the function of TLR4 homologs across all fishes remains debatable. Recent work suggests zebrafish Tlr4 mediates ototoxic responses to a platinum-based chemotherapeutic. This prompts our hypothesis that Tlr4 detects group IX/X transition metals and thus has conserved roles with human TLR4 mediating allergic responses to nickel. Here, we use the larval zebrafish lateral line model to demonstrate (sub-)micromolar Ni, Co and Pt are ototoxic in a dose-dependent manner. TLR4 homologs are required for this toxicity because Tlr4 knockdown via CRISPR significantly reduced the metals' impacts by ~50%. Moreover, zebrafish Tlr4 was sufficient to mediate inflammatory responses to metals when expressed in a human cell line. These data show zebrafish TLR4 homologs are necessary and sufficient to mediate responses to metals, however, direct biophysical binding of metals to zebrafish TLR4 homologs remains uninvestigated. These data are consistent with the notion that mediating responses to transition metals was a function of TLR4 homologs in the last common ancestor of fish and mammals, and begins to resolve the function(s) of TLR4 homologs in the zebrafish animal model of disease.

KEYWORDS

toll-like receptor 4, MD-2, innate immunity, ecotoxicology, inflammation

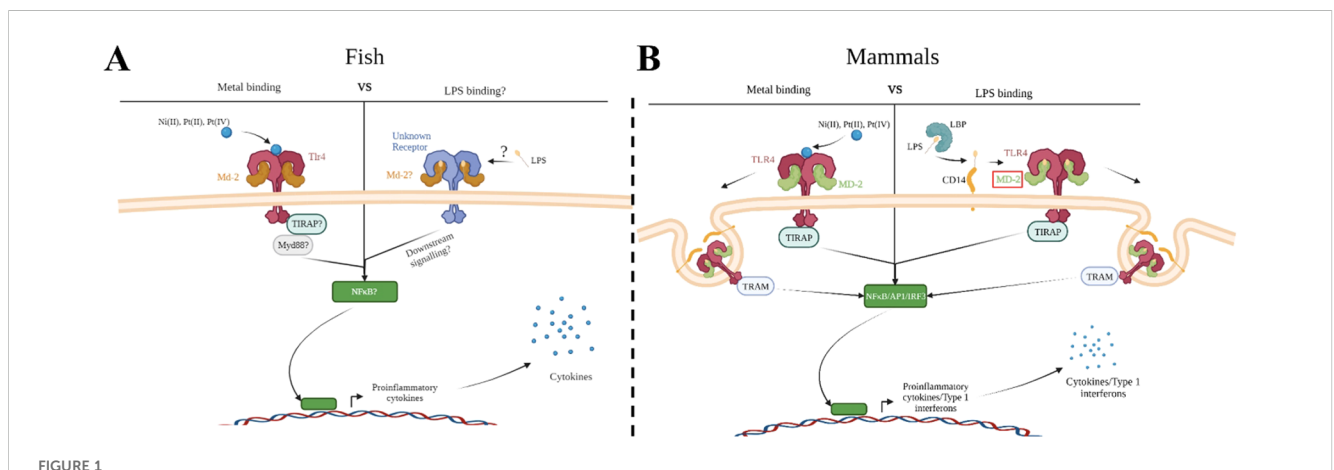
# 1 Introduction

Toll-like receptors (TLRs) are evolutionarily ancient proteins with origins dating back to more than 700 MYA and can be found in a range of organisms from corals to humans (1, 2). Mammalian TLR4 is multifaceted in its function with involvement in pathogen recognition, cancer pathology, and autoimmune disease (3). The best studied function of TLR4 in humans is its ability to detect and bind to microbial pathogen associated molecular patterns (PAMPs) such as lipopolysaccharide (LPS), and viral glycoproteins, which are essential for the body's inflammatory response to pathogens. The structure of TLR4 is conserved between species, however the function of TLR4 homologs in zebrafish (and in all fish and other early-branching vertebrates) has remained elusive. This has potential to frustrate interpretations when using zebrafish as an important model of disease, and so we seek to fill that knowledge gap here.

TLR4 proteins can be classified as pattern recognition receptors (PRRs), and like all PRRs they act as the sentinels of the innate immune system, surveying the host environment for signs of foreign molecules and alarming the host to damage or foreign bodies. Mammalian TLR4's primary ligand is LPS, an important extracellular component of the cell wall in Gram-negative bacteria. In zebrafish, however, no convincing evidence demonstrates that LPS signals via TLR4; although LPS has impacts when applied to zebrafish (often only at extra-biologic high concentrations, and in screening efforts to discover phytobiologicals) as demonstrated in scores of papers (4–13), these impacts of LPS have not been shown to require TLR4. The reason for the disparity between TLR4 signaling in mammals and fish may be attributed to TLR4 itself and/or to the evolution of the associated intracellular signaling pathways (14–19), or perhaps the

appropriate source of LPS has yet to be tested. In mammals, signaling through TLR4 using LPS requires multiple different coreceptors acting in concert with one another including: LPS binding protein (LBP), cluster differentiation 14 (CD14), and myeloid differentiation factor 2 (MD-2) (20). Activation of TLR4 leads to downstream signaling and initiation of pro-inflammatory and type 1 interferon related gene expression through NF-κB and IRF3 respectively (Figure 1). Dysfunction in any of these signaling components has been demonstrated to impede the proper functioning of TLR4 as a bacterial sensor (21). Recently, the homolog for MD-2 was discovered in zebrafish, prompting Loes et al. to reconsider Tlr4's role in LPS recognition and signaling within zebrafish (2021). Although Loes et al. found the zebrafish homolog Tlr4ba was capable of being activated by high concentrations of LPS, it's low sensitivity to LPS and the lack of other crucial co-receptors in the zebrafish genome suggests zebrafish Tlr4 primarily recognizes other unidentified ligands. MD-2 contributes to signaling through LPS, but it also plays a role in signaling through other TLR4 ligands such as metals. Overall, the detection of LPS via TLR4 appears to have evolved in mammals after that lineage split from other vertebrates, and thus the function of TLR4 in fishes, including those related to important models of disease, has remained elusive (17).

The observation that metals, such as nickel, can act as ligands of TLR4 was a crucial discovery in determining the involvement of the innate immune system in mediating metal contact hypersensitivity, a type of allergic contact dermatitis (ACD) (22). Two mechanisms are believed to play a role during the sensitization of the immune system to nickel (23). One mechanism involves the generation of an adaptive immune response following first contact with the allergen, while the other mechanism is through the activation of innate immune cells via TLR4 (23–25). Similar to LPS, metal binding to



Metal ion activation of zebrafish TIr4 and direct binding to human TLR4 versus co-receptor binding with LPS. Group IX/X transition metals activate a proinflammatory response through zebrafish toll-like receptor 4 (TIr4) (A) or human TLR4 (B). (A) Metal ions activate a proinflammatory response through zebrafish TLR4 homologs, which may be mediated through myeloid differentiation factor 2 (Md-2). Activation would likely lead to signaling through downstream molecules, such as myeloid differentiation primary response 88 (Myd88), leading to activation of a proinflammatory transcription factor (such as nuclear factor- $\kappa\beta$  (NF- $\kappa\beta$ )) and release of proinflammatory cytokines. LPS signaling in zebrafish remains unclear but would likely involve a similar signaling cascade as described above. (B) Metal ions bind directly to key residues in the ectodomain of human TLR4 leading to dimerization and binding of MD-2. This stimulates nuclear factor- $\kappa\beta$  (NF- $\kappa\beta$ ) and interferon regulatory transcription factor 3 (IRF3), leading to the release of type 1 interferons and proinflammatory cytokines. LPS binds to the LPS Binding Protein (LBP) and is transferred to the coreceptor cluster of differentiation 14 (CD14). CD14 facilitates the binding of LPS to MD-2/TLR4 signaling complex, which then dimerizes and follows a similar signaling cascade as described above. Created with BioRender.

TLR4 leads to the production of pro-inflammatory cytokines, recruiting immune cells and generating inflammation resulting in itching, tenderness, swelling, and rashes (25, 26). However, metal binding to TLR4 is through a distinct mechanism that doesn't require the co-receptors associated with LPS signaling (27–29) (Figure 1). Metals bind directly to the ectodomain of TLR4 leading to TLR4 dimerization through a cluster of conserved histidine residues (28, 30). Oblak et al. determined MD-2 was only needed for stabilization of the TLR4 complex during metal ion binding after dimerization and allows for downstream signaling through the MyD88-dependent and -independent pathways (2015). Taken together, we were motivated to investigate metals as potential ligands of zebrafish Tlr4 homologs (31).

Zebrafish are a potent model organism for the study of human disease and have gained recognition as an excellent model for immunological processes (32, 33) and drug discovery (11, 34, 35). They allow for examination of cellular interaction at a wholeorganism level and possess many of the same innate immune components as humans (32, 36). Zebrafish possess a total of 20 TLRs and express three TLR4 homologs known as Tlr4ba, Tlr4bb, and Tlr4al. Unlike mammalian TLR4, zebrafish Tlr4 has not been demonstrated to respond to LPS, and zebrafish lack the co-receptor CD14. LPS is a modular structure that can be capped by an Oantigen, referred to as "smooth" LPS, where CD14 is required for TLR4 activation by smooth LPS in mammals (17, 37, 38). Nevertheless, zebrafish TLR4 proteins are structurally congruent with their mammalian counterparts, with all three homologs coding for an extracellular leucine-rich repeat (LRR) ectodomain, a transmembrane domain and a toll/interleukin-1 receptor (TIR) containing domain (39) (Supplementary Figure 1). Moreover, Loes et al. has recently uncovered the existence of a zebrafish Md-2 homolog that interacts with Tlr4ba, providing evidence of an ancestral interaction between Tlr4 and Md-2 facilitating the detection of extracellular ligands (2021). In chimeric TLR4 fusion experiments, their transmembrane and TIR domains have also shown to function in a similar manner to mammals, capable of eliciting a proinflammatory response after activation (38). Furthermore, Purcell et al. showed zebrafish and humans possess many of the same intracellular signaling molecules such as MyD88, TIRAP, TRIF, TRAF6, IRF3, and IRF7 40. The difference in their ligand specificity appears to lie within the ectodomain, with Tlr4ba, Tlr4al, and Tlr4bb proteins showing ~36% identity to the ectodomain of human TLR4 respectively (Supplementary Figure 2).

The lack of a known primary ligand for zebrafish Tlr4 is puzzling as they appear to have all the components required for sensing an extracellular ligand, yet their true function is still a mystery. Our previous studies have shown zebrafish Tlr4 to be involved in cisplatin-induced ototoxicity (41). Morpholino knockdown of *tlr4ba* and *tlr4bb* mitigated cell death induced by the platinum (II) based chemotherapeutic cisplatin (41). This observation, and the unique mechanism of TLR4 activation by metals in mammals, led us to hypothesize that group IX/X transition metals are a ligand of TLR4 that predates the evolutionary split between fish and mammals. Thus, we predict that group IX/X transition metals will initiate zebrafish Tlr4

activation, leading to NF $\kappa\beta$  induction and a proinflammatory response. Here, we present Ni (II), Co (II), Pt (II) and Pt (IV) as novel activators and potential ligands of zebrafish Toll-like receptor 4 (Tlr4). The findings improve the understanding of Tlr4 evolution, and ultimately advance the utility of zebrafish as an animal model for future studies in innate immunity and disease.

# 2 Methods

# 2.1 Zebrafish husbandry and ethics

Zebrafish were kept in standard conditions at the University of Alberta aquatics facility following a 14:10 light/dark cycle in 28.5°C. They were fed twice daily using either trout chow or brine shrimp. All zebrafish were raised, bred, and maintained following the institutional Animal Care and Use Committee approved protocol AUP00000077 which operates under guidelines set by the Canadian Council of Animal Care.

# 2.2 Zebrafish breeding and care

Wildtype (AB strain) zebrafish were bred and maintained at 28.5°C in standard conditions (42). Embryos were maintained in E3 media containing 0.01% methylene blueE3 media was made from a 60X stock solution of embryo media (prepared with 0.29M NaCl, 0.01M KCl, 0.026M CaCl<sub>2</sub>, 0.001M MgSO<sub>4</sub>• 7H<sub>2</sub>O) diluted to 1X in Milli-Q water or mixed with 0.01% methylene blue solution in a 5.5:1 ratio before being diluted in Milli-Q water. Embryos were grown in a 28.5°C incubator and the E3 media was replaced daily.

# 2.3 Metal ion treatment of larval zebrafish

Wildtype (AB strain) zebrafish larvae were grown to either 5- or 6-days post fertilization (dpf) in E3 embryo media with methylene blue and 10-15 larvae were placed in each well of a six-well plate. The larvae were then bath treated with either 0, 2.5, 5, 7.5, 10, or 15μM of nickel (II) (Sigma; prod. #654507) or cobalt (II) (Sigma; prod. #255599) chloride hexahydrate or 0, 0.25, 0.5, 0.75, 1, or  $1.5\mu M$  of platinum (II) (Sigma; prod. #206091) or platinum (IV) (Sigma; prod. #206113) chloride diluted in E3 media with methylene blue for 20 hours at 28°C. All wells were then washed with embryo media three times before being incubated on an orbital incubator shaker at 130 rpm and 28°C for 15-20 minutes in media containing 0.01% 2-[4-(dimethylamino) styryl]-1-ethylpyridinium iodide (DASPEI, Sigma Aldrich; cat. #3785-01-1) to selectively stain live neuromast hair cells. The wells were washed twice using E3 media and groups of larvae were transferred into individual petri dishes where they were anaesthetized using 4% Tricaine-S (MS-222). After blinding the researcher to treatments, the neuromasts were imaged using a Leica M165 FC dissecting microscope equipped with a GFP-long pass fluorescent filter.

# 2.4 Neuromast quantification assay

The DASPEI quantification assay has been established by many studies, but the one used here was modified from Babolmorad et al. (2021; 43–46). Briefly, five neuromasts along the posterior lateral line were chosen for scoring consistently throughout experiments (Figure 2). Each neuromast was assigned a score ranging from 0–2 based on fluorescent intensity. A score of 2 is assigned to bright neuromasts with no noticeable decline in fluorescence, 1.5 for minor decline, 1 for moderate decline, 0.5 for severe decline and 0 for complete loss of fluorescence. The neuromast viability score for each larva was determined by calculating the sum of these five scores, with a total maximum score of 10. A lower score represents a decline in neuromasts health (indicative of ototoxicity), while a higher score (near 10) represents healthy neuromasts.

# 2.5 Guide RNA design and injections

Previous work has shown that the biallelic editing ability of clustered regularly interspaced short palindromic repeats (CRISPR)-cas9 technology allows for the generation of F0 "crispant" knockdowns in a target gene with high fidelity (>80%) (47-51). This approach allows for high throughput examination of loss-of-function phenotypes within zebrafish larvae with reduced number of resources and time. Knockdown of TLR4 homologs (the generation of tlr4 "crispants"), used duplexes of trans-activating CRISPR-RNA (tracrRNA) and CRISPR-RNA (crRNA) to produce a single guide RNA (sgRNA). The cas9 nuclease binds to the tracrRNA and is guided to mutate the target gene through the crRNA. crRNAs for tlr4ba, tlr4al, and tlr4bb were designed using the predesigned Alt-R® CRISPR-Cas9 guide RNA program offered by Integrated DNA Technologies (IDT). The crRNA sequences used can be found in Supplementary Table 1. The final gRNAs for each gene were made by mixing 100µM of the tracrRNA and 100µM of the crRNA, heating them to 95°C for 5 minutes, and diluting them to 25µM using the nuclease-free duplex buffer (IDT; cat. #11-05-01-12). All three gRNAs (25μM) were combined along with Cas9 protein (25µM) and heated to 37°C for 10 minutes to make a ribonuclease complex (25µM, RNP). The injection solution contained RNP (25µM), 1% dextran tetramethylrhodamine (invitrogen; cat. #D1817), 1M KCl, and RNAse-free water filled to 10µL. Wildtype (AB) zebrafish embryos at the 1 cell stage were injected with either a mock solution containing only the Cas-9 protein (mock injected) or the injection solution containing gRNAs (tlr4ba/al/bb crispant). Injected embryos were then incubated at 28.5°C in E3 media.

At 1 dpf dead embryos were removed from the petri dish and E3 media was replaced with fresh media. At 2 dpf embryos were screened for the injection using a Leica M165 FC dissecting microscope equipped with an mCherry fluorescent filter. Injected embryos showing red fluorescence were sorted and grown to 5 dpf at 28.5°C.

# 2.6 Confirming efficacy of tlr4 CRISPR via genotyping

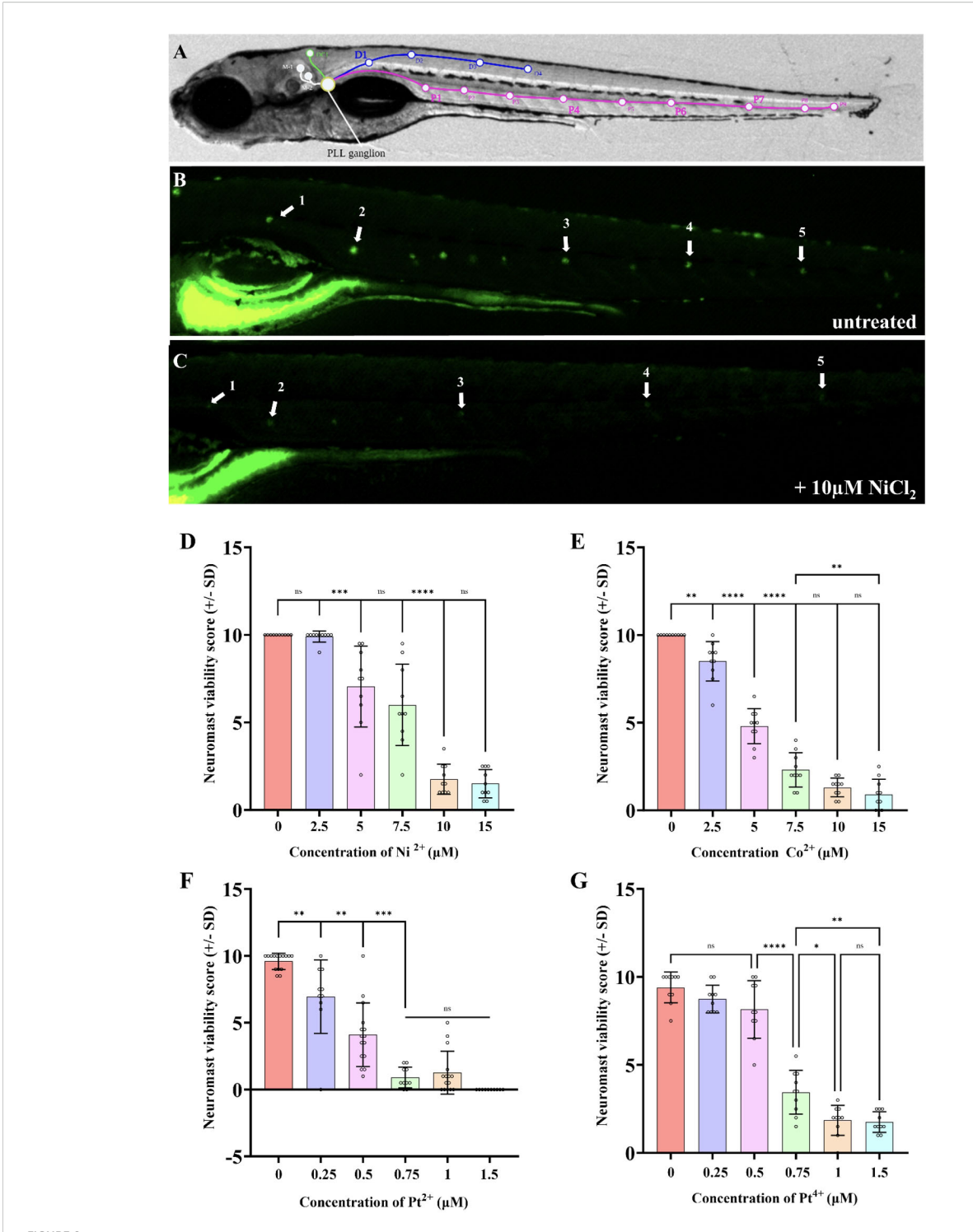
A standard genomic DNA extraction was done on all uninjected, mock and tlr4ba/al/bb CRISPR injected larvae that were scored during metal experiments. The extraction was performed by submerging whole larvae in 15µL of 50µM NaOH and boiling them in the thermocycler at 95°C for 15 minutes, followed by a cooling period of 4°C for 5 minutes. 5µL Tris-HCl was added to neutralize the solution and DNA was stored at 4°C. A PCR was performed on genomic DNA samples using the AllTaq<sup>TM</sup> Master Mix Kit (Qiagen; cat. #203146) following the manufacturer's protocol. PCR product concentration was then quantified using a Nanodrop 2000 spectrophotometer (Thermo Scientific). Primers used for the PCR amplification of each zebrafish tlr4 homolog can be found in Supplementary Table 1. Thermocycling conditions were a 2 minute denaturing period at 95°C, then a specific amplification period for five cycles of 94°C for 15 seconds, 64°C for 15 seconds, and 72°C for 30 seconds, followed by a less-specific amplification for 30 cycles of 94°C for 15 seconds, 54 °C for 15 seconds, and 72°C for 30 seconds, and a final extension at 72°C for 10 minutes. Finally, Sanger-sequencing using the same PCR primer sets was performed on the amplified tlr4ba, tlr4al, and tlr4bb genes from 1 uninjected, 1 mock injected and 5 tlr4 mutant larvae chosen at random.

# 2.7 HEK293T cell transfection and treatment

Human embryonic kidney (HEK) 293T cells (ATCC, catalog (cat) number CRL-3216) were grown in Dulbecco's Modified Eagle Medium (DMEM) supplemented with FBS (10%) and penicillinstreptomycin (100 µg/mL) at 37°C and 5% CO<sub>2</sub>. Cells were seeded in 24-well plates (5 x 10<sup>4</sup> cells/well) for functional assays and 6-well plates (5 x 10<sup>5</sup> cells/well) for immunoblotting. 24 hours after seeding, the HEK293T cells were transfected with an empty vector (pcDNA3-2xHA) or co-transfected with zebrafish Tlr4ba, Tlr4bb (a generous gift from Dr. Victoriano Mulero, Spain) (37), or a human TLR4 expression clone (Addgene, cat. #13018). Additionally, an empty vector or human MD-2 (OriGene, cat. #RC204686) were transiently expressed. Transfections were done following the manufacturer's protocol using jetPRIME reagent (Polyplus, cat. #CA89129-924) with half the indicated amount of DNA. The media in each well was replaced with fresh media 4 hours post-transfection. 48 hours post-transfection, media was aspirated, and the cells were treated with nickel (II) chloride hexahydrate (Sigma, cat. #379840), or LPS (Invitrogen, cat. #L23351) diluted in fresh media.

# 2.8 Western blot analysis of zebrafish Tlr4 expression

Transfected cells were placed on ice for 5–10 minutes, washed with ice-cold PBS, and returned to ice. Cells were lysed using 200  $\mu$ L



Nickel (II) chloride, cobalt (II) chloride, platinum (II) chloride, and platinum (IV) chloride induce PLL hair cell death in a dose dependent manner within 6-7dpf zebrafish. (A) Location of posterior lateral line neuromasts drawn on a bright field image of a 7dpf larva. (B) DASPEI stained untreated larva with visible neuromasts. White arrows indicate the neuromasts that were consistently selected for scoring between experiments. (C) DASPEI stained larva treated with 10μM nickel (II) chloride hexahydrate, showing the significant decline in neuromast fluorescence due to hair cell death. White arrows indicate the selected neuromasts relative to those selected in panel (A). A "neuromast viability score" was calculated for each individual that assigned a score to the aforementioned five neuromasts (exemplar in panel B score is 10, exemplar in panel C score is 3) as described in the methods; a score of 10 is normal and lower scores indicate lower neuromast health/viability. As the concentration of the NiCl<sub>2</sub> (D), CoCl<sub>2</sub> (E), PtCl<sub>2</sub> (F), and PtCl<sub>4</sub> (G) in the media increased, the neuromast hair cell viability decreased. NiCl<sub>2</sub> and CoCl<sub>2</sub> were less toxic to neuromast hair cells compared to platinum salts. N = 10 wildtype larvae for all treatment groups. Bars represent the mean neuromast viability score of all larvae, whiskers display the standard deviation (SD) and each dot represents data from an individual larva. \*\*\*\*p<0.001, \*\*\*p<0.001, \*\*p<0.005, ns = not significant by one way ANOVA and Tukey's multiple comparison test.

of cold Modified Oncogene Science Lysis Buffer [MOSLB; 10 mM HEPES at pH 7.4, 50 mM Na Pyrophosphate, 50 mM NaF, 50 mM NaCl, 5 mM EDTA, 5 mM EGTA, 100 µM Na<sub>3</sub>VO<sub>4</sub>, 1% Triton X-100, Roche protease inhibitor cocktail (Sigma, cat. #11697498001); kindly provided by the Marchant group, UofA MMI) and by rocking for 15-20 minutes. The wells were rinsed with the lysis buffer and the lysates were collected in pre-chilled microcentrifuge tubes. The lysates were centrifuged at 4°C for 10 minutes at 6000g and then the supernatants were collected in new pre-chilled tubes. Lysates were mixed with 6X Laemmli buffer at a 1:5 (buffer:lysate) ratio and then the samples were loaded without heating and separated on a 10% SDS-PAGE gel before transfer to a nitrocellulose membrane. The membrane was blocked with LiCor Intercept (TBS) Blocking Buffer for 1 hour at room temperature, then probed with mouse anti-V5 antibody (1:5000) (Invitrogen, cat. #R96025) overnight at 4°C, and then probed with goat anti-mouse secondary antibody (1:5000) (LiCor, IRDye 800CW) for 1 hour at room temperature. The membrane was washed with TBST and imaged on a LiCor Odyssey.

# 2.9 HEK293T cell viability and IL-8 secretion

IL-8 cytokine secretion relative to no agonist treatment was used as a measure of TLR4 in these cells. Supernatants were collected 24 hours post-treatment and then IL-8 secretion was quantified using commercial human IL-8 ELISA kits (Invitrogen, cat. #88-8086) according to the manufacturer's protocol. IL-8 secretion was normalized to cell viability to account for cell death by nickel. Cell viability was measured using MTT reagent (3-(4,5-dimethylthiazol-2-yl)-2,5-diphenyl tetrazolium bromide) (ACROS, cat. #158990010). MTT was diluted to 1 mg/mL in fresh media and added to the cells post-treatment and incubated for 4 hours. Formazan was solubilized in DMSO (dimethyl sulfoxide) (Sigma, cat. #276855) and then the absorbance was measured at 590 nm on a SpectraMAX i3x plate reader (Molecular Devices).

# 2.10 Phylogenetic and synteny analysis of zebrafish Tlr4

A phylogenetic reconstruction analysis of TLR4 was performed in MEGA11 as described (Hall et al., (52, 53). Briefly, multiple protein sequences from different vertebrates with e-values <0.001 were collected from NCBI through a BLASTp of zebrafish Tlr4ba in MEGA11. A multiple sequence alignment was performed using MUSCLE under the default options. To determine the most appropriate model for sequence evolution under maximum likelihood (ML) for this data set, we used MEGA's program to find the best model for estimating the tree. The Nearest-Neighborinterchange (NNI) algorithm was used to generate initial unrooted tree(s) for the heuristic search, which was estimated using the JJT+F+G+I substitution model with 1000 bootstrap replications (54). All positions with less than 95% site coverage were eliminated, i.e.,

fewer than 5% alignment gaps, missing data, and ambiguous bases were allowed at any position.

Synteny analysis was performed using the Genomicus 93.01 available at: https://www.genomicus.bio.ens.psl.eu/genomicus-93.01/cgi-bin/search.pl. The gene tree was rooted at the duplication of Tlr4 in early vertebrates. All Tlr4 sequences are collected from the Ensembl database, with all low-coverage sequences removed from the tree. Species for comparison were then selected for analysis.

# 2.11 Statistical analysis

Individual neuromast scores for each larva were added together to provide a neuromast viability score for each individual animal, and this score was used for subsequent analysis. The mean neuromast viability scores and hair cell counts from each group were analyzed using one-way ANOVA with Tukey's multiple comparisons test. The  $EC_{50}$  for metal ion data was calculated by normalizing each data set, followed by a non-linear regression with a variable slope. When the data was normalized, 0% and 100% of a response was defined as the smallest and largest mean in each data set respectively. All graphs and statistical tests were performed using GraphPad Prism 9. HEK293T normalized IL-8 secretion values were analyzed using an RM two-way ANOVA and Tukey's multiple comparisons test.

# 3 Results

# 3.1 Nickel, cobalt, and platinum induce hair cell death in larval zebrafish neuromast hair cells

In mammals, nickel is known to induce allergic contact hypersensitivity reactions through the direct binding and activation of TLR4 (22, 28). Other group X transition metals, such as platinum, have recently been shown to activate mammalian TLR4 through a similar mechanism as nickel (27). Previous findings show Tlr4 signaling is highly conserved between mammals and zebrafish, with the lowest conservation area being within the extracellular domain (38, 55) (Supplementary Figure 2). This difference, along with lack of co-receptors, is believed to contribute to the low sensitivity of zebrafish Tlr4 homologs to LPS. Instead, we speculate zebrafish Tlr4 might be suitable for the direct binding of metal ions. Indeed, we recently established that a platinum-based chemical is toxic to zebrafish neuromast hair cells in a manner that requires zebrafish TRL4 homologs (41), so we reasoned that hair cell health could be a favorable proxy of zebrafish Tlr4 mediating metal toxicity in vivo. We examined the ototoxicity of NiCl2, CoCl2, PtCl2, and PtCl4 and found a monophasic dosedependent relationship between neuromast viability and metal ion concentration (Figure 2). The EC<sub>50</sub> of neuromast viability for NiCl<sub>2</sub>, CoCl<sub>2</sub>, PtCl<sub>2</sub>, and PtCl<sub>4</sub> was found to be 7.6µM, 4.6µM, 0.44µM, and 0.64µM respectively, demonstrating the high toxicity of

platinum salts to hair cells (Supplementary Figure 3). PtCl<sub>2</sub> had a >10-fold toxicity to the pLL neuromasts in comparison to NiCl<sub>2</sub>, which was the least toxic metal compound (Figures 2D, F). Group IX/X transition metals did not appear to have any overt morphological effects on larvae over the course of treatment (applied for 20 hours at 5–6 dpf; Supplementary Figure 4). Together, these results demonstrate that the tested group IX/X transition metals induce dose-dependent neuromast hair cell death in larval zebrafish.

# 3.2 Zebrafish TLR4 homologs are required for metal toxicity in PLL neuromast hair cells

To test whether the cytotoxic effects on neuromast hair cells from nickel and platinum require zebrafish Tlr4, we used CRISPR-Cas9 gene editing technology to produce crispant larvae where all three zebrafish tlr4 genes (tlr4ba, tlr4al, and tlr4bb) were targeted for mutagenesis. Crispant larva were established by injecting a Cas9/gRNA ribonuclear complexes (RNPs) targeting a sequence early in tlr4ba, tlr4al, and tlr4bb gene homologs (Supplementary Figure 5). The "mock" injected larvae received Cas9 protein but not the gRNA duplex and were used as a control for any effects of the microinjection process. CRISPR efficacy was confirmed by sequencing the tlr4 genes. As expected, Sanger sequencing showed no detectable mutations within the tlr4 genes of

uninjected or mock injected larvae, while crispant larvae had non-consensus sequences beginning in their tlr4ba and tlr4bb genes at positions that exactly aligned with CRISPR gRNA binding sites, indicating genome cleavage and variable mutations products (Supplementary Figures 6-8). This confirmed that the tlr4ba and tlr4bb genes were successfully disrupted in crispants. The status of tlr4al in crispants is ambiguous insomuch that sequencing of several larvae failed to reveal mutations, but the position of the tlr4al gene in between tlr4ba and tlr4bb genes on Chromosome 13 (Supplementary Figure 5) leaves open the possibility that this chromosomal region may have been disrupted in select individuals. From this we cannot determine conclusively if tlr4al plays any role in our outcomes. Crispant larvae displayed no overt phenotypes compared to uninjected, or mock injected larva prior to application of metals (Supplementary Figure 3).

We used these tlr4 crispants to test the hypothesis that zebrafish TLR4 homologs are required for mediating the metal toxicity observed in hair cells. Knockdown of TLR4 homologs protected hair cells from metal toxicity (Figure 3). Treatment with  $10\mu M$  NiCl2,  $0.75\mu M$  PtCl2 or  $0.75\mu M$  PtCl4, led to significantly less damage to neuromast hair cells in crispants compared to controls (Figure 3). The mutations in tlr4ba and tlr4bb resulted in a greater than 2-fold increase in mean neuromast viability after treatment with nickel and platinum compounds in comparison to uninjected larva, demonstrating the involvement of zebrafish Tlr4 in metal induced neuromast hair cell toxicity.

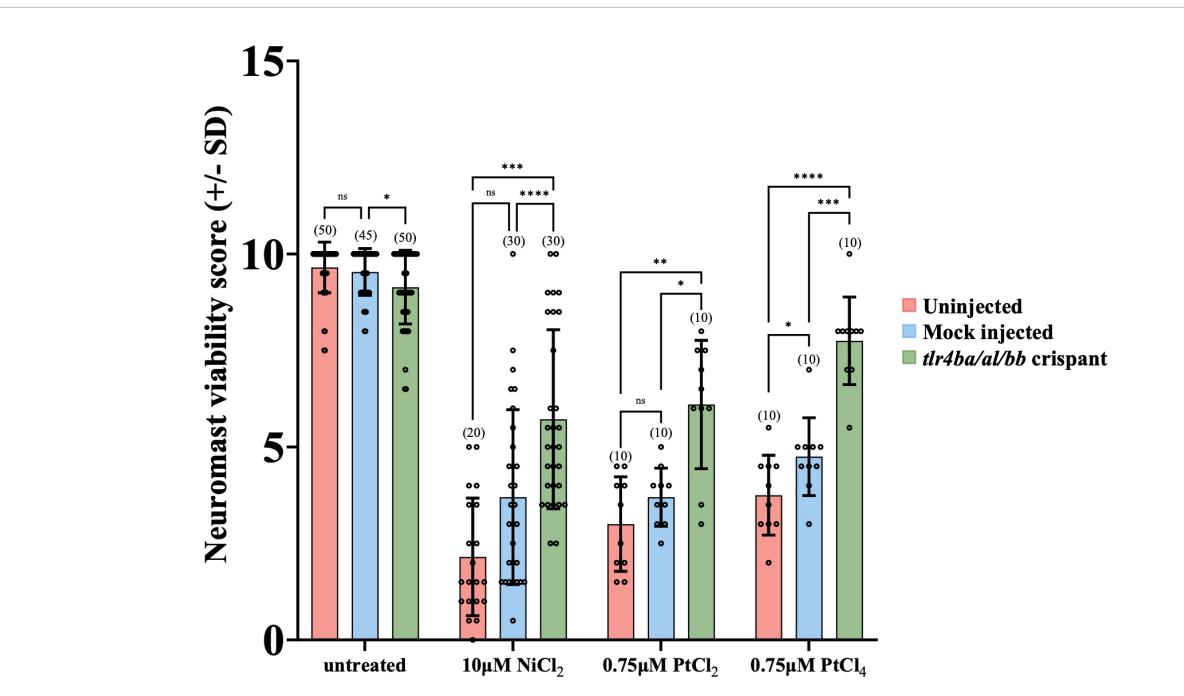


FIGURE 3 ttr4 crispant mutant larvae are less susceptible to Group 10 transition metal induced ototoxicity. Both uninjected and mock injected larvae show a significant decrease in neuromast hair cell survival after treatment with  $10\mu M$  NiCl<sub>2</sub> and  $0.75\mu M$  PtCl<sub>2</sub> and PtCl<sub>4</sub>. The ttr4 crispant larvae had their ttr4 homologs mutated, protecting them from group 10 transition metal induced ototoxicity. Neuromast viability scores of ttr4 crispants were significantly higher than mock and uninjected nickel and platinum treated groups. Larvae were mutated in their ttr4 homologs using CRISPR-cas9 genome editing. Larvae were injected at the single-cell stage with either gRNA sequences targeting the three zebrafish ttr4 homologs or Cas9 protein alone (mock). Larvae were treated with cisplatin for 20 hours at 6 dpf. Bracketed numbers above each bar represents the total number of larvae scored in each group. \*p<0.05; \*\*p<0.01; \*\*\*\*p<0.001; \*\*\*\*p<0.0001, ns = not significant by one way ANOVA and Tukey's multiple comparison test.

# 3.3 Zebrafish Tlr4 transfected into HEK293T cells show a modest response to nickel, but no measurable response to LPS

HEK293T cells do not normally express TLR4 but can be rendered responsive to TLR4 agonists when transfected with human TLR4 and MD-2 – they have been shown to upregulate proinflammatory gene expression in response to known TLR4 agonists (27, 41, 56–58). IL-8 has been established by numerous studies as a marker for TLR4 activation making HEK293T cells an appropriate *in vitro* cell model to assess TLR4 function (22, 30, 59–62).

Transient expression of human *TLR4* in our HEK cell-based system conferred responsiveness to nickel and LPS, in an MD-2 dependent manner, serving as a positive control for TLR4 activation in this system (Figure 4A). When similarly expressed, both zebrafish TLR4 homologs *tlr4ba* or *tlr4bb* were sufficient to mediate signaling to nickel (Figures 4B, C), approximately doubling the response. Stable expression of zebrafish homologs in the HEK cell system was confirmed by immunoblot (Supplementary Figure 9). Zebrafish homologs of TLR4 showed no measurable response to LPS (despite co-expression of human *MD-2*), consistent with past reports (37, 38).

# 4 Discussion

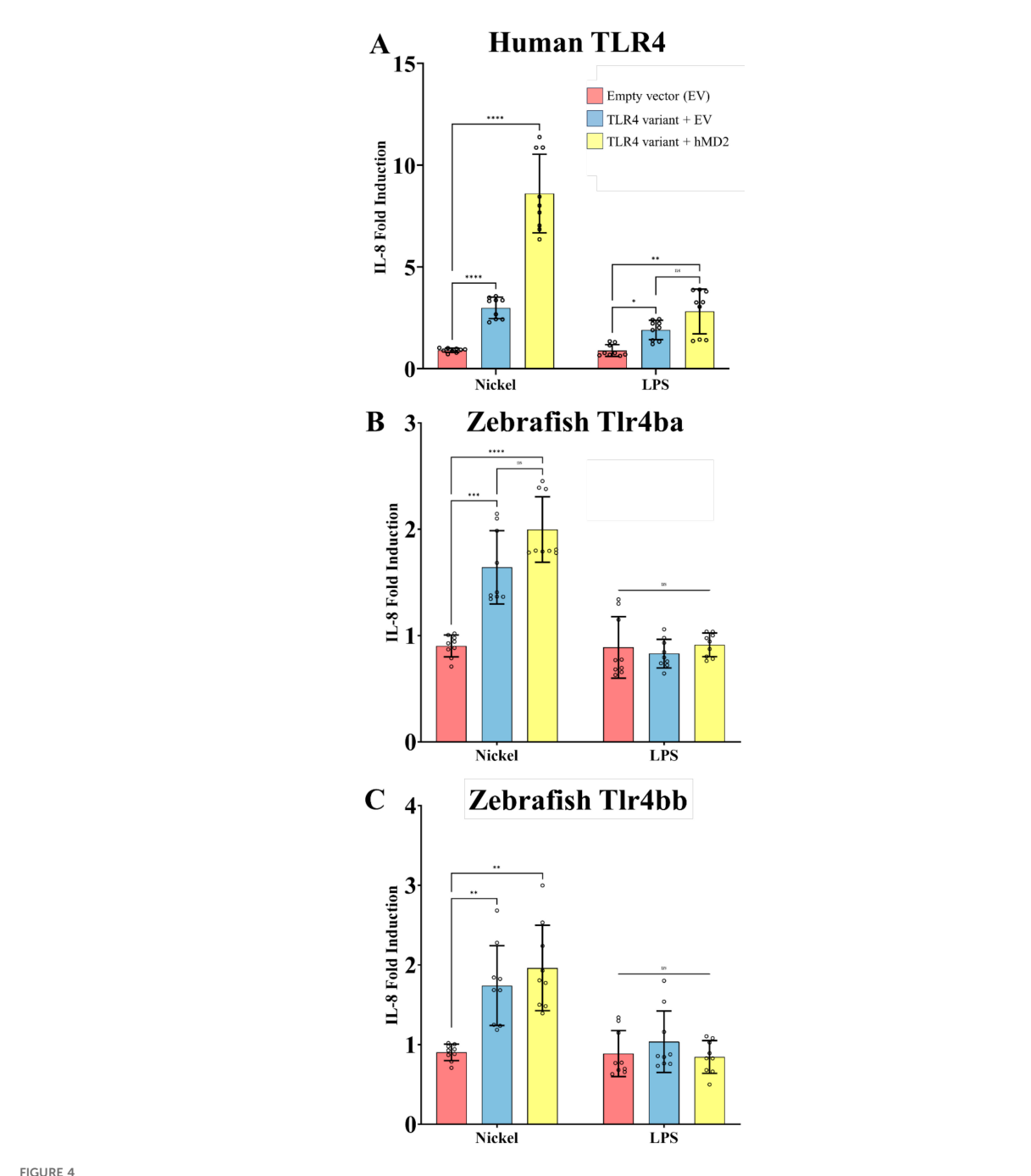
This study demonstrates that group IX/X transition metals mediate the activation of zebrafish homologs of TLR4, providing insight to the long-standing mystery of TLR4 function in early-branching vertebrates. We showed that bath application of NiCl<sub>2</sub>, CoCl<sub>2</sub>, PtCl<sub>2</sub>, or PtCl<sub>4</sub> impacted the viability of neuromast hair cells and that this effect required zebrafish homologs of TLR4. Furthermore, zebrafish Tlr4ba or Tlr4bb were capable of transducing signals following nickel treatment when expressed in a heterologous cell platform. Altogether, this data suggests zebrafish homologs of TLR4 mediate cellular responses to metal ions, which is a response previously observed only in mammals (including humans and closely related primates).

Exposure to trace metals such as nickel, cobalt, zinc, and copper has been previously observed to induce inflammatory responses in zebrafish (63, 64). Metal ions induce expression of proinflammatory cytokines such as  $il1\beta$  and  $tnf\alpha$  as well as Tlr signaling genes myd88, nfkb1a, and tlr5b (65-67). The involvement of Tlrs in mediating these inflammatory responses is further supported by the observation that the MAPK pathway also shows increased gene expression after metal exposure (66). In humans, metals elicit these responses described above through the binding and activation of TLR4 (22, 30, 41, 68). Additionally, as observed in humans following metal-induced TLR4 activation, contact with metal ions in zebrafish can lead to the development of high concentrations of reactive oxygen species (ROS), leading to further inflammation, disruption of mitochondrial function, and eventually cell death (67, 69). In this study we show that during bath application with metal ions, clusters of hair cells on the exterior of zebrafish, called neuromasts, aptly demonstrate the ability of metals to induce cell death. This effect can be mitigated by mutations in Tlr4ba/Tlr4bb, resulting in a reduction of metal cytotoxicity. This data provides evidence that the generation of metal-induced cell death in zebrafish is mediated in some part through the activity of Tlr4 homologs.

These findings provide further support to our hypothesis that zebrafish Tlr4 can be activated by metals, and while this suggests an ancient, shared function for vertebrate TLR4 it also raises new questions about how previous works align with this conclusion. The binding of nickel to human TLR4 has been shown to be directly mediated through two histidine residues within the LRR domain. These residues are conserved between primate species such as chimpanzees and humans but are largely absent in more distantly related vertebrates (22, 28). Previously, it has been suggested that due to the lack of these histidine residues, other species apart from primates fail to respond to metal ions through TLR4 (22, 30). Mice have demonstrated nickel hypersensitivity through TLR4 activation, but only when pre-sensitized with LPS as an adjuvant (70). In contrast, our findings show that cells transfected with zebrafish Tlr4 homologs increase secretion of IL-8 in response to nickel and in the absence of LPS, similar to what is seen in humans (22, 68). Furthermore, MD-2 was not required for metal induced activation of zebrafish Tlr4, suggesting a binding mechanism like that observed in humans. Further work is warranted towards understanding which residues in zebrafish Tlr4 mediate metal signaling. Regardless, this implicates zebrafish as a promising animal model for studying metal allergies and provides an in vivo system to examine the complexity of metal-induced contact hypersensitivity reactions and future therapeutic avenues.

Human TLR4 is a promiscuous receptor known to be activated by a variety of ligands beyond LPS and nickel, including one of its most important functions: recognition of cellular damage following the release of damage-associated molecular patterns (DAMPs). Metal ions may result in the release of DAMPs into the media, which then mediate the activation of zebrafish Tlr4 homologs. Therefore, we cannot rule out the possibility of DAMPs as a confound within this study. However, the activation of hTLR4 by some DAMPS such as HMGB1, requires co-receptors such as MD-2, which is not required for IL-8 secretion by cells expressing zebrafish Tlr4 (71). Furthermore, to our knowledge zebrafish Tlr4 homologs have only one endogenous ligand, but examining endogenous activators of zebrafish Tlr4 provides an exciting avenue for future study. For example, Liu et al. showed that peroxiredoxin 1, a widely expressed antioxidant enzyme and DAMP, could interact with Tlr4ba, inducing NF-κB activity and upregulating expression of proinflammatory cytokines (72, 73). This finding supports some role of DAMPs in zebrafish Tlr4 activation, however more work is required to determine the role DAMPs play in metal induced Tlr4 activation in zebrafish.

The ability of zebrafish Tlr4, particularly Tlr4ba, to respond to LPS was recently re-visited by Loes et al. after their insightful observation of an MD-2 homolog present within the zebrafish genome (2021). LPS was shown to be capable of activating zebrafish Tlr4ba in the presence of MD-2, however, there are two caveats: it required mammalian Cd14, which currently has no



Nickel activates zebrafish Tlr4 homologs when expressed in a heterologous system. HEK293T cells transiently expressing TLR4 homologs from human (A) and zebrafish (Tlr4ba and Tlr4bb, in panels B and C, respectively) with and without MD-2 were treated with the potential TLR4 agonists nickel (200  $\mu$ M) or LPS (10 ng/mL). (A) Human TLR4 confers responsiveness to Ni or LPS agonists, as measured via IL-8 secretion, showing LPS is active and serving as a benchmark comparator for zebrafish homologs. (B, C) Zebrafish Tlr4ba and Tlr4bb confer responsiveness to nickel as assessed by IL-8 secretion, but are largely independent of MD-2 expression. Data are presented as the fold increase relative to untreated isogenic samples. N = three independent experiments for all treatments, and each N is the mean of technical replicates. \*\*\*\*p<0.0001, \*\*\*p<0.0002, \*\*p<0.00332, ns = not significant by two-way RM ANOVA and Šídák's multiple comparisons test. .

known homolog within zebrafish, and the concentrations required for activation of zebrafish Tlr4 were considerably higher ( $\mu g/mL$ ) than the biologically relevant concentrations of LPS (0-10ng/mL) required for TLR4 activation (74). Importantly, LPS has complex variations between sources and preparations; Further exploration is

needed to determine if LPS sourced from fish pathogens might be better able to initiate signaling of fish TLR4 homologs.

On the other hand, dimerization by metal ions is through a direct binding mechanism and excludes the aforementioned prerequisite of CD14 for activation. The presence of Tlr4

homologs and an MD-2 homolog within zebrafish, along with LPS sensitivity being undetectable, provided the logical basis for our hypothesis that zebrafish Tlr4 utilizes group IX/X metals for ligands. The most recent hypotheses for how zebrafish Tlr4 fits in to the evolution of this receptor suggests the *tlr4* gene along with *ly96* (MD-2) arose in a common ancestor before divergence of lobe-finned and ray-finned fish (31). The lack of a CD14 homolog, and the ill-defined LPS sensitivity in most fish species, further supports the notion that Tlr4's purpose originally included the binding of ligands that do not require co-receptors, such as metals.

In summary, we present data in support of nickel and platinum acting as novel ligands for zebrafish Tlr4, helping discern the mystery surrounding the function of TLR4 across evolutionary time. We demonstrate that genetic mutation of Tlr4 renders zebrafish significantly less sensitive to metals, whereas zebrafish homologs of TLR4 when expressed in heterologous cells were sufficient to induce an inflammatory response to metals. These findings suggest a previously unknown function of zebrafish Tlr4, which includes detecting metals in their environment or physiology. We anticipate that an improved understanding of the function of zebrafish Tlr4 and its involvement with metal ions will facilitate better utilization of this model organism in the study of innate immunity and the myriad of various diseases involving inflammation, particularly including metal contact hypersensitivity.

# Data availability statement

The original contributions presented in the study are included in the article/Supplementary Material. Further inquiries can be directed to the corresponding author.

# **Ethics statement**

The animal study was approved by Animal Care and Use Committee: BioSciences at the University of Alberta. The study was conducted in accordance with the local legislation and institutional requirements.

# Author contributions

AF: Formal Analysis, Investigation, Methodology, Writing – original draft, Writing – review & editing. TL: Formal Analysis, Investigation, Methodology, Writing – review & editing. SM: Investigation, Methodology, Validation, Writing – review & editing. NP: Methodology, Writing – review & editing. AL: Supervision, Formal analysis, Investigation, Writing – review & editing. AB: Conceptualization, Funding acquisition, Project administration, Supervision, Writing – review & editing. WA: Conceptualization, Funding acquisition, Supervision, Writing – review & editing.

# **Funding**

The author(s) declare financial support was received for the research and/or publication of this article. Funding was from operating grants to APB and WTA from CIHR (PJT-178327). Funders played no role in design or interpretation of the experiments.

# Acknowledgments

Victoriano Mulero kindly provided plasmids for expression of zebrafish homologs of zebrafish TLR4. Operating grants to APB and WTA from CIHR (PJT-178327). Studentship to TSL from the Cancer Research Institute of Northern Alberta. We appreciate support of animal wellbeing provided by Science Animal Support Services at the University of Alberta. Chris Li assisted with generation of gRNA sequences as well as PCR primers for crispant validation.

# Conflict of interest

The authors declare that the research was conducted in the absence of any commercial or financial relationships that could be construed as a potential conflict of interest.

# Generative AI statement

The author(s) declare that no Generative AI was used in the creation of this manuscript.

Any alternative text (alt text) provided alongside figures in this article has been generated by Frontiers with the support of artificial intelligence and reasonable efforts have been made to ensure accuracy, including review by the authors wherever possible. If you identify any issues, please contact us.

# Publisher's note

All claims expressed in this article are solely those of the authors and do not necessarily represent those of their affiliated organizations, or those of the publisher, the editors and the reviewers. Any product that may be evaluated in this article, or claim that may be made by its manufacturer, is not guaranteed or endorsed by the publisher.

# Supplementary material

The Supplementary Material for this article can be found online at: https://www.frontiersin.org/articles/10.3389/fimmu.2025.1679375/full#supplementary-material

SUPPLEMENTARY FIGURE 1

Multiple sequence alignment and percent identity matrix for TLR4 (full protein) between zebrafish, mice, and humans. (A) The comparison

between sequences shows the homology and conservation of residues mainly in the latter third of the protein sequence. Similar residues (100%) are highlighted in black, partially similar residues are highlighted in dark grey (80%-100%) and light grey (60%-80%). The colored histogram shows the mean pairwise percent identity for each column of the alignment, where green represents 100%, yellow represents >30%, and red represents <30%. (B) Table shows the percent sequence identity between mammalian TLR4 (mouse and human) is >60%, while the percent identity between mammalian and zebrafish Tlr4 homologs is <40%. Alignments, similarity, and the percent identity matrix were made and calculated using Geneious Prime.

#### SUPPLEMENTARY FIGURE 2

Multiple sequence alignment and percent identity matrix for TLR4 extracellular LRR domain and intracellular TIR domain between human, mouse, and zebrafish. The comparison between extracellular LRR domain (A, B) sequences shows the homology and conservation of residues is ~20% greater within the intracellular TIR domain (C, D) compared with the extracellular LRR domain. Similar residues (100%) are highlighted in black, partially similar residues are highlighted in dark grey (80%-100%) and light grey (60%-80%). The colored histogram shows the mean pairwise percent identity for each column of the alignment, where green represents 100%. yellow represents >30%, and red represents <30%. The known human nickel binding residues are underlined in red within (A). The nickel binding residues 431 and 456 show 100% similarity between humans, mice, and zebrafish, as well as partial identity (>30%) and consist of either histidine or tyrosine residues. The last known nickel binding residue (458) shows low similarity and identity between all sequence and is either a histidine, asparagine, serine, or arginine residue. The tables (B, D) below the alignments (A, C) show the percent sequence identity for the entire sequence alignment between human TLR4, mouse TLR4, zebrafish Tlr4ba, Tlr4al, and Tlr4bb. Alignments, similarity, and the percent identity matrix were made and calculated using Geneious Prime.

### SUPPLEMENTARY FIGURE 3

Normalized linear regression plots of nickel, cobalt, platinum II, and platinum IV dose response curves. Neuromast viability responses to varying concentrations of NiCl $_2$  (A), CoCl $_2$  (B), PtCl $_2$  (C), and PtCl $_4$  (D) were averaged and normalized where 0% and 100% of a response was defined as the smallest and largest mean in each data set respectively. EC $_{50}$  values were then calculated using a non-linear regression with variable slope in GraphPad Prism 10.

# SUPPLEMENTARY FIGURE 4

Tlr4 crispant fish treated with nickel (II) and platinum (IV). (A, C) 6-7dpf mock injected and Tlr4 crispant larva treated with either PtCl<sub>4</sub> or NiCl<sub>2</sub> show no apparent morphological change in comparison to an uninjected untreated larva. (A) Uninjected, untreated larva. (B) Mock injected larva treated with 7.5 $\mu$ M PtCl<sub>4</sub>. (C) Tlr4 crispant treated with 7.5 $\mu$ M PtCl<sub>4</sub>. (D) Mock injected larva treated with 10 $\mu$ M NiCl<sub>2</sub>. (E) Tlr4 crispant larva treated with 10 $\mu$ M NiCl<sub>2</sub>.

# SUPPLEMENTARY FIGURE 5

Illustration representing the three *TLR4* homologs on zebrafish chromosome 13 and their approximate gRNA positions. The three zebrafish *tlr4* homologs are found in succession to one another. Arrows point to the initial base pair position on the chromosome. White boxes represent untranslated regions,

blue boxes represent exons, while blue lines denote introns. Grey lines represent the intergenic region connecting the homologs.

#### SUPPLEMENTARY FIGURE 6

Sanger Sequencing of tlr4ba crispant DNA. The *tlr4ba* gene was amplified from the genomic DNA of individual larvae via PCR using the tlr4ba forward primer. Uninjected larva (A) and mock injected larva (B) DNA shows an unmutated *tlr4ba* sequence, where consistent DNA in all cells produces a coherent chromatogram throughout. (C) Chromatograms from *tlr4* cripants show consensus sequence chromatograms where the DNA is homozygous and consistent throughout the individual (left side), but the chromatogram becomes discrepant from wild type sequence near the gRNA binding site (highlighted in red) because a mixture of various mutant DNA sequences now exists among the larva's cells. Larvae were injected at the single-cell stage with either a gRNA sequence targeting the zebrafish tlr4ba homolog or Cas9 protein alone (mock).

#### SUPPLEMENTARY FIGURE 7

Sanger Sequencing of tlr4bb crispant DNA. The *tlr4bb* gene was amplified from the genomic DNA of individual larvae via PCR using the *tlr4bb* reverse primer. Uninjected larva (A) and mock injected larva (B) DNA shows an unmutated *tlr4bb* sequence, where consistent DNA in all cells produces a coherent chromatogram throughout. (C) Chromatograms from *tlr4* crispants show consensus sequence chromatograms where the DNA is homozygous and consistent throughout the individual (left side), but the chromatogram becomes discrepant from wild type sequence near the gRNA binding site (highlighted in red) because a mixture of various mutant DNA sequences now exists among the larva's cells. Larvae were injected at the single-cell stage with either a gRNA sequence targeting the zebrafish tlr4bb homolog or Cas9 protein alone (mock).

## SUPPLEMENTARY FIGURE 8

Sanger Sequencing of tlr4al crispant DNA. The  $\it tlr4al$  gene was amplified from the genomic DNA of individual larvae via PCR using the  $\it tlr4al$  reverse primer. Uninjected larva (A) and mock injected larva (B) DNA in A & B shows an unmutated  $\it tlr4al$  sequence, where consistent DNA in all larval cells produces a coherent chromatogram throughout. (C) Chromatograms from  $\it tlr4$  cripants show consensus sequence chromatograms where the DNA is homozygous and consistent throughout the individual even following the gRNA target sequence (highlighted in red).

# SUPPLEMENTARY FIGURE 9

Zebrafish Tlr4ba and Tlr4bb are stably produced in HEK293T cells. Top: Zebrafish *tlr4ba* and *tlr4bb* were transiently expressed in HEK293T cells from a constitutive promoter. A signal of the expected size was observed in cells transiently expressing V5/His<sub>6</sub>-epitope tagged zebrafish Tlr4 proteins (zfTlr4ba, zfTlr4bb). Lysate from cells transiently expressing V5-tagged ASC was used as a positive control, while lysates from non-transfected (nt) or empty vector (EV)-transfected HEK293T cells were used as negative controls. Bottom: Human TLR4 is stably expresses in HEK293T cells. Cells were transfected with hTLR4-YFP. Lysates were probed with anti-GFP primary antibody and only lysates from transfected cells showed signal, whereas HEK293T cells alone did not

# SUPPLEMENTARY TABLE 1

CRISPR-cas9 gRNA sequences and PCR primer sequences.

# References

- 1. Behzadi P, Garcia-Perdomo HA, Karpinski TM. Toll-like receptors: general molecular and structural biology. *J Immunol Res.* (2021) 2021:9914854. doi: 10.1155/2021/9914854
- 2. Fitzgerald KA, Kagan JC. Toll-like receptors and the control of immunity. Cell. (2020) 180:1044–66. doi: 10.1016/j.cell.2020.02.041
- 3. Heine H, Zamyatina A. Therapeutic targeting of TLR4 for inflammation, infection, and cancer: A perspective for disaccharide lipid A mimetics. *Pharm (Basel)*. (2022) 16. doi: 10.3390/ph16010023
- 4. Athapaththu AMGK, Lee KT, Kavinda MHD, Lee S, Kang S, Lee MH, et al. Pinostrobin ameliorates lipopolysaccharide (LPS)-induced inflammation and
- endotoxemia by inhibiting LPS binding to the TLR4/MD2 complex. Biomed Pharmacother. (2022) 156:113874. doi: 10.1016/j.biopha.2022.113874
- 5. Bates JM, Akerlund J, Mittge E, Guillemin K. Intestinal alkaline phosphatase detoxifies lipopolysaccharide and prevents inflammation in zebrafish in response to the gut microbiota. *Cell Host Microbe*. (2007) 2:371–82. doi: 10.1016/j.chom.2007.10.010
- 6. Fernando IPS, Sanjeewa KKA, Samarakoon KW, Lee WW, Kim HS, Kang N, et al. A fucoidan fraction purified from Chnoospora minima; a potential inhibitor of LPS-induced inflammatory responses. *Int J Biol Macromol.* (2017) 104:1185–93. doi: 10.1016/j.ijbiomac.2017.07.031

- 7. Hwang JH, Kim KJ, Ryu SJ, Lee BY. Caffeine prevents LPS-induced inflammatory responses in RAW264.7 cells and zebrafish. *Chem Biol Interact.* (2016) 248:1–7. doi: 10.1016/j.cbi.2016.01.020
- 8. Lee SH, Ko CI, Jee Y, Jeong Y, Kim M, Kim JS, et al. Anti-inflammatory effect of fucoidan extracted from Ecklonia cava in zebrafish model. *Carbohydr Polym.* (2013) 92:84–9. doi: 10.1016/j.carbpol.2012.09.066
- 9. Li W, Luo F, Wu X, Fan B, Yang M, Zhong W, et al. Anti-inflammatory effects and mechanisms of dandelion in RAW264.7 macrophages and zebrafish larvae. *Front Pharmacol.* (2022) 13:906927. doi: 10.3389/fphar.2022.906927
- $10.~Urzi\ O,$  Cafora M, Ganji NR, Tinnirello V, Gasparro R, Raccosta S, et al. Lemonderived nanovesicles achieve antioxidant and anti-inflammatory effects activating the AhR/Nrf2 signaling pathway. <code>iScience.</code> (2023) 26:107041. doi: 10.1016/j.isci.2023.107041
- 11. Yang LL, Wang GQ, Yang LM, Huang ZB, Zhang WQ, Yu LZ. Endotoxin molecule lipopolysaccharide-induced zebrafish inflammation model: a novel screening method for anti-inflammatory drugs. *Molecules*. (2014) 19:2390–409. doi: 10.3390/molecules19022390
- 12. Yu GR, Lim DW, Karunarathne W, Kim GY, Kim H, Kim JE, et al. A non-polar fraction of Saponaria officinalis L. acted as a TLR4/MD2 complex antagonist and inhibited TLR4/MyD88 signaling *in vitro* and in *vivo*. *FASEB J*. (2022) 36:e22387. doi: 10.1096/fj.202200018RR
- 13. Zhang P, Wang H, Hong Y, Yu M, Zeng R, Long Y, et al. Selective visualization of endogenous hypochlorous acid in zebrafish during lipopolysaccharide-induced acute liver injury using a polymer micelles-based ratiometric fluorescent probe. *Biosens Bioelect.* (2018) 99:318–24. doi: 10.1016/j.bios.2017.08.001
- 14. Candel S, Sepulcre MP, Espín-Palazón R, Tyrkalska SD, de Oliveira S, Meseguer J, et al. Md1 and Rp105 regulate innate immunity and viral resistance in zebrafish. *Dev Comp Immunol.* (2015) 50:155–65. doi: 10.1016/j.dci.2015.01.005
- 15. Candel S, Tyrkalska SD, Garcia-Moreno D, Meseguer J, Mulero V. Identification of Evolutionarily Conserved Md1 Splice Variants That Regulate Innate Immunity through Differential Induction of NF-small ka, CyrillicB. *J Immunol.* (2016) 197:1379–88. doi: 10.4049/jimmunol.1502052
- 16. Liu Y, Li M, Fan S, Lin Y, Lin B, Luo F, et al. A unique feature of toll/IL-1 receptor domain-containing adaptor protein is partially responsible for lipopolysaccharide insensitivity in zebrafish with a highly conserved function of myd88. *J Immunol.* (2010) 185:3391–400. doi: 10.4049/jimmunol.0903147
- 17. Martinez-Lopez A, Tyrkalska SD, Alcaraz-Perez F, Cabas I, Candel S, Martinez Morcillo FJ, et al. Evolution of LPS recognition and signaling: The bony fish perspective. *Dev Comp Immunol.* (2023) 145:104710. doi: 10.1016/j.dci.2023.104710
- 18. Novoa B, Bowman TV, Zon L, Figueras A. LPS response and tolerance in the zebrafish (Danio rerio). Fish Shellfish Immunol. (2009) 26:326–31. doi: 10.1016/j.fsi.2008.12.004
- 19. Palti Y. Toll-like receptors in bony fish: from genomics to function. *Dev Comp Immunol.* (2011) 35:1263–72. doi: 10.1016/j.dci.2011.03.006
- 20. Ryu J-K, Kim SJ, Rah S-H, Kang JI, Jung HE, Lee D, et al. Reconstruction of LPS transfer cascade reveals structural determinants within LBP, CD14, and TLR4-MD2 for efficient LPS recognition and transfer. *Immunity*. (2017) 46:38–50. doi: 10.1016/j.immuni.2016.11.007
- 21. Ciesielska A, Matyjek M, Kwiatkowska K. TLR4 and CD14 trafficking and its influence on LPS-induced pro-inflammatory signaling. *Cell Mol Life Sci.* (2021) 78:1233–61. doi: 10.1007/s00018-020-03656-y
- 22. Schmidt M, Raghavan B, Müller V, Vogl T, Fejer G, Tchaptchet S, et al. Crucial role for human Toll-like receptor 4 in the development of contact allergy to nickel. *Nat Immunol.* (2010) 11:814–9. doi: 10.1038/ni.1919
- 23. Riedel F, Aparicio-Soto M, Curato C, Thierse HJ, Siewert K, Luch A. Immunological mechanisms of metal allergies and the nickel-specific TCR-pMHC interface. *Int J Environ Res Public Health*. (2021) 18. doi: 10.3390/ijerph182010867
- 24. De Graaf NPJ, Roffel S, Gibbs S, Kleverlaan CJ, Lopez Gonzalez M, Rustemeyer T, et al. Nickel allergy is associated with a broad spectrum cytokine response. *Contact Dermati.* (2023) 88:10–7. doi: 10.1111/cod.14199
- 25. Saito M, Arakaki R, Yamada A, Tsunematsu T, Kudo Y, Ishimaru N. Molecular mechanisms of nickel allergy. *Int J Mol Sci.* (2016) 17:202. doi: 10.3390/ijms17020202
- 26. Katsnelson A. Nickel allergy tracked to a single receptor. *Nature*. (2010). doi: 10.1038/news.2010.407
- 27. Domingo IK, Groenendyk J, Michalak M, Bhavsar AP. Cisplatin toxicity is mediated by direct binding to toll-like receptor 4 through a mechanism that is distinct from metal allergens. *Mol Pharmacol.* (2023) 103:158–65. doi: 10.1124/molpharm.122.000595
- 28. Peana M, Zdyb K, Medici S, Pelucelli A, Simula G, Gumienna-Kontecka E, et al. Ni(II) interaction with a peptide model of the human TLR4 ectodomain. *J Trace Elements Med Biol.* (2017) 44:151–60. doi: 10.1016/j.jtemb.2017.07.006
- 29. Raghavan B, Martin SF, Esser PR, Goebeler M, Schmidt M. Metal allergens nickel and cobalt facilitate TLR4 homodimerization independently of MD2. *EMBO Rep.* (2012) 13:1109–15. doi: 10.1038/embor.2012.155
- 30. Oblak A, Pohar J, Jerala R. MD-2 determinants of nickel and cobalt-mediated activation of human TLR4. *PloS One*. (2015) 10:e0120583. doi: 10.1371/journal.pone.0120583

- 31. Loes AN, Hinman MN, Farnsworth DR, Miller AC, Guillemin K, Harms MJ. Identification and characterization of zebrafish tlr4 coreceptor md-2. *J Immunol*. (2021) 206:1046–57. doi: 10.4049/jimmunol.1901288
- 32. Gomes MC, Mostowy S. The case for modeling human infection in zebrafish. Trends Microbiol. (2020) 28:10–8. doi: 10.1016/j.tim.2019.08.005
- 33. van der Sar AM, Appelmelk BJ, Vandenbroucke-Grauls CM, Bitter W. A star with stripes: zebrafish as an infection model. *Trends Microbiol.* (2004) 12:451–7. doi: 10.1016/j.tim.2004.08.001
- 34. Patton EE, Zon LI, Langenau DM. Zebrafish disease models in drug discovery: from preclinical modelling to clinical trials. *Nat Rev Drug Discov.* (2021) 20:611–28. doi: 10.1038/s41573-021-00210-8
- 35. Stewart AM, Braubach O, Spitsbergen J, Gerlai R, Kalueff AV. Zebrafish models for translational neuroscience research: from tank to bedside. *Trends Neurosci.* (2014) 37:264–78. doi: 10.1016/j.tins.2014.02.011
- 36. Novoa B, Figueras A. Zebrafish: model for the study of inflammation and the innate immune response to infectious diseases. *Adv Exp Med Biol.* (2012) 946:253–75. doi: 10.1007/978-1-4614-0106-3 15
- 37. Sepulcre MP, Alcaraz-Pérez F, López-Muñoz A, Roca FJ, Meseguer J, Cayuela ML, et al. Evolution of lipopolysaccharide (LPS) recognition and signaling: fish TLR4 does not recognize LPS and negatively regulates NF-κB activation. *J Immunol.* (2009) 182:1836–45. doi: 10.4049/jimmunol.0801755
- 38. Sullivan C, Charette J, Catchen J, Lage CR, Giasson G, Postlethwait JH, et al. The Gene History of Zebrafish tlr4a and tlr4b Is Predictive of Their Divergent Functions1. *J Immunol.* (2009) 183:5896–908. doi: 10.4049/jimmunol.0803285
- 39. Vaure C, Liu Y. A comparative review of toll-like receptor 4 expression and functionality in different animal species. *Front Immunol.* (2014) 5:316. doi: 10.3389/fimmu.2014.00316
- 40. Purcell MK, Smith KD, Hood L, Winton JR, Roach JC. Conservation of toll-like receptor signaling pathways in teleost fish. Comp Biochem Physiol Part D Genomics Proteomics. (2006) 1:77–88. doi: 10.1016/j.cbd.2005.07.003
- 41. Babolmorad G, Latif A, Domingo IK, Pollock NM, Delyea C, Rieger AM, et al. Toll-like receptor 4 is activated by platinum and contributes to cisplatin-induced ototoxicity. *EMBO Rep.* (2021) 22:e51280. doi: 10.15252/embr.202051280
- 42. Westerfield M. The zebrafish book. A guide for the laboratory use of zebrafish (Danio rerio). 5th Edition. Eugene, OR: University of Oregon Press (2007).
- 43. Coffin AB, Reinhart KE, Owens KN, Raible DW, Rubel EW. Extracellular divalent cations modulate aminoglycoside-induced hair cell death in the zebrafish lateral line. *Hearing Res.* (2009) 253:42–51. doi: 10.1016/j.heares.2009.03.004
- 44. Harris JA, Cheng AG, Cunningham LL, MacDonald G, Raible DW, Rubel EW. Neomycin-induced hair cell death and rapid regeneration in the lateral line of zebrafish (Danio rerio). *J Assoc Res Otolaryngol.* (2003) 4:219–34. doi: 10.1007/s10162-002-3022-x
- 45. Owens KN, Cunningham DE, Macdonald G, Rubel EW, Raible DW, Pujol R. Ultrastructural analysis of aminoglycoside-induced hair cell death in the zebrafish lateral line reveals an early mitochondrial response. *J Comp Neurol.* (2007) 502:522–43. doi: 10.1002/cne.21345
- 46. Uribe PM, Villapando BK, Lawton KJ, Fang Z, Gritsenko D, Bhandiwad A, et al. Larval zebrafish lateral line as a model for acoustic trauma. *eNeuro*. (2018) 5. doi: 10.1523/ENEURO.0206-18.2018
- 47. Burger A, Lindsay H, Felker A, Hess C, Anders C, Chiavacci E, et al. Maximizing mutagenesis with solubilized CRISPR-Cas9 ribonucleoprotein complexes. *Development.* (2016) 143:2025–37. doi: 10.1242/dev.134809
- 48. Hoshijima K, Jurynec MJ, Klatt Shaw D, Jacobi AM, Behlke MA, Grunwald DJ. Highly efficient CRISPR-cas9-based methods for generating deletion mutations and F0 embryos that lack gene function in zebrafish. *Dev Cell.* (2019) 51:645–657 e644. doi: 10.1016/j.devcel.2019.10.004
- 49. Jao L-E, Wente SR, Chen W. Efficient multiplex biallelic zebrafish genome editing using a CRISPR nuclease system. *Proc Natl Acad Sci.* (2013) 110:13904–9. doi: 10.1073/pnas.1308335110
- 50. Kroll F, Powell GT, Ghosh M, Gestri G, Antinucci P, Hearn TJ, et al. A simple and effective F0 knockout method for rapid screening of behaviour and other complex phenotypes. *eLife*. (2021) 10:e59683. doi: 10.7554/eLife.59683
- 51. Shah AN, Davey CF, Whitebirch AC, Miller AC, Moens CB. Rapid reverse genetic screening using CRISPR in zebrafish. *Nat Methods*. (2015) 12:535–40. doi: 10.1038/nmeth.3360
- 52. Hall BG. Building phylogenetic trees from molecular data with MEGA. *Mol Biol Evol.* (2013) 30:1229–35. doi: 10.1093/molbev/mst012
- 53. Tamura K, Stecher G, Kumar S. MEGA11: molecular evolutionary genetics analysis version 11. *Mol Biol Evol*. (2021) 38:3022–7. doi: 10.1093/molbev/msab120
- 54. Jones DT, Taylor WR, Thornton JM. The rapid generation of mutation data matrices from protein sequences. *Bioinformatics*. (1992) 8:275–82. doi: 10.1093/bioinformatics/8.3.275
- 55. Zhang J, Kong X, Zhou C, Li L, Nie G, Li X. Toll-like receptor recognition of bacteria in fish: Ligand specificity and signal pathways. *Fish Shellfish Immunol.* (2014) 41:380–8. doi: 10.1016/j.fsi.2014.09.022
- 56. Chow JC, Young DW, Golenbock DT, Christ WJ, Gusovsky F. Toll-like receptor-4 mediates lipopolysaccharide-induced signal transduction. *J Biol Chem.* (1999) 274:10689–92. doi: 10.1074/jbc.274.16.10689

57. Medvedev AE, Vogel SN. Overexpression of CD14, TLR4, and MD-2 in HEK 293T cells does not prevent induction of *in vitro* endotoxin tolerance. *J Endotoxin Res.* (2003) 9:60–4. doi: 10.1177/09680519030090010801

- 58. Yang H, Young DW, Gusovsky F, Chow JC. Cellular events mediated by lipopolysaccharide-stimulated toll-like receptor 4. MD-2 is required for activation of mitogen-activated protein kinases and Elk-1. *J Biol Chem.* (2000) 275:20861–6. doi: 10.1074/jbc.M002896200
- 59. Kurt-Jones EA, Popova L, Kwinn L, Haynes LM, Jones LP, Tripp RA, et al. Pattern recognition receptors TLR4 and CD14 mediate response to respiratory syncytial virus. *Nat Immunol.* (2000) 1:398–401. doi: 10.1038/80833
- 60. McKee HK, Kajiwara C, Yamaguchi T, Ishii Y, Shimizu N, Ohara A, et al. Clostridioides difficile toxins enhanced the *in vitro* production of CXC chemokine ligand 2 and tumor necrosis factor-α via Toll-like receptors in macrophages. *J Med Microbiol.* (2021) 70. doi: 10.1099/jmm.0.001342
- 61. Potnis PA, Dutta DK, Wood SC. Toll-like receptor 4 signaling pathway mediates proinflammatory immune response to cobalt-alloy particles. *Cell Immunol.* (2013) 282:53–65. doi: 10.1016/j.cellimm.2013.04.003
- 62. Quevedo-Diaz MA, Song C, Xiong Y, Chen H, Wahl LM, Radulovic S, et al. Involvement of TLR2 and TLR4 in cell responses to Rickettsia akari. *J Leukoc Biol.* (2010) 88:675–85. doi: 10.1189/jlb.1009674
- 63. Juśkiewicz W, Gierszewski P. Toxic metal pollution of aquatic ecosystems of European Union nature protection areas in a region of intensive agriculture (Lake Gopło, Poland). *Aquat Sci.* (2022) 84:52. doi: 10.1007/s00027-022-00884-1
- 64. Singh V, Singh N, Rai SN, Kumar A, Singh AK, Singh MP, et al. Heavy Metal Contamination in the Aquatic Ecosystem: Toxicity and Its Remediation Using Eco-Friendly Approaches. *Toxics*. (2023) 11:147. Available online at: https://www.mdpi.com/2305-6304/11/2/147.
- 65. Brun NR, Koch BEV, Varela M, Peijnenburg WJGM, Spaink HP, Vijver MG. Nanoparticles induce dermal and intestinal innate immune system responses in zebrafish embryos [10.1039/C8EN00002F. Environ Sci: Nano. (2018) 5:904–16. doi: 10.1039/C8EN00002F

- 66. Chen M, Luo Y, Xu J, Chang M-X, Liu J-X. Copper regulates the susceptibility of zebrafish larvae to inflammatory stimuli by controlling neutrophil/macrophage survival [Original research. *Front Immunol.* (2019) 10:2599. doi: 10.3389/fimmu.2019.02599
- 67. Wang T, Long X, Liu Z, Cheng Y, Yan S. Effect of copper nanoparticles and copper sulphate on oxidation stress, cell apoptosis and immune responses in the intestines of juvenile Epinephelus coioides. *Fish Shellfish Immunol.* (2015) 44:674–82. doi: 10.1016/j.fsi.2015.03.030
- 68. Rachmawati D, Bontkes HJ, Verstege MI, Muris J, Von Blomberg BME, Scheper RJ, et al. Transition metal sensing by Toll-like receptor-4: next to nickel, cobalt and palladium are potent human dendritic cell stimulators. *Contact Dermati.* (2013) 68:331–8. doi: 10.1111/cod.12042
- 69. Jia D, Zhang R, Shao J, Zhang W, Cai L, Sun W. Exposure to trace levels of metals and fluoroquinolones increases inflammation and tumorigenesis risk of zebrafish embryos. *Environ Sci Ecotechnol.* (2022) 10:100162. doi: 10.1016/j.ese.2022.100162
- 70. Sato N, Kinbara M, Kuroishi T, Kimura K, Iwakura Y, Ohtsu H, et al. Lipopolysaccharide promotes and augments metal allergies in mice, dependent on innate immunity and histidine decarboxylase. *Clin Exp Allergy.* (2007) 37:743–51. doi: 10.1111/j.1365-2222.2007.02705.x
- 71. Yang H, Wang H, Ju Z, Ragab AA, Lundbäck P, Long W, et al. MD-2 is required for disulfide HMGB1–dependent TLR4 signaling. J Exp Med. (2015) 212:5–14. doi: 10.1084/jem.20141318
- 72. He Y, Li S, Tang D, Peng Y, Meng J, Peng S, et al. Circulating Peroxiredoxin-1 is a novel damage-associated molecular pattern and aggravates acute liver injury via promoting inflammation. *Free Radical Biol Med.* (2019) 137:24–36. doi: 10.1016/j.freeradbiomed.2019.04.012
- 73. Liu G-p, Xiang L-x, Shao T, Lin A-f, Shao J-z. Stimulatory function of peroxiredoxin 1 in activating adaptive humoral immunity in a zebrafish model. *Dev Comp Immunol.* (2018) 84:353–60. doi: 10.1016/j.dci.2018.03.004
- 74. Guo S, Al-Sadi R, Said HM, Ma TY. Lipopolysaccharide causes an increase in intestinal tight junction permeability *in vitro* and *in vivo* by inducing enterocyte membrane expression and localization of TLR-4 and CD14. *Am J Pathol.* (2013) 182:375–87. doi: 10.1016/j.ajpath.2012.10.014